3D face recognition based on matching of facial surfaces

Beatriz Adriana Echeagaray-Patrón, Vitaly Kober

Beatriz Adriana Echeagaray-Patrón, Vitaly Kober, "3D face recognition based on matching of facial surfaces," Proc. SPIE 9598, Optics and Photonics for Information Processing IX, 95980V (9 September 2015); doi: 10.1117/12.2186695

SPIE.

Event: SPIE Optical Engineering + Applications, 2015, San Diego, California, United States

3D face recognition based on matching of facial surfaces

Beatriz Adriana Echeagaray-Patrón[a]* and Vitaly Kober[a,b]**

[a]Department of Computer Science, CICESE, Ensenada, B.C. 22860, Mexico
[b]Department of Mathematics, Chelyabinsk State University, Russian Federation

ABSTRACT

Face recognition is an important task in pattern recognition and computer vision. In this work a method for 3D face recognition in the presence of facial expression and poses variations is proposed. The method uses 3D shape data without color or texture information. A new matching algorithm based on conformal mapping of original facial surfaces onto a Riemannian manifold followed by comparison of conformal and isometric invariants computed in the manifold is suggested. Experimental results are presented using common 3D face databases that contain significant amount of expression and pose variations.

Keywords: 3D face recognition, 3D facial shape analysis, conformal mapping.

1. INTRODUCTION

Face Recognition is a problem that has remained relevant in recent years due to its wide range of applications such as access control, surveillance, human-computer interaction, and biometric identification systems. Despite the variety of techniques that have been developed, the problem remains open: accurate and robust face recognition still offers a number of challenges, especially under unconstrained and uncontrolled environments.

Several studies have shown that the use of data from 3D scans can improve face recognition especially in the presence of illumination changes. Nevertheless, range images still have undesirable variations owing to pose variations. When working with a single 3D camera, the facial surface is not fully independent of posture because the camera has a limited field of view. This issue decreases significantly the performance of recognition algorithms if the partial surface view is not taken into account. A popular way in 3D face recognition of posture correction is based on surface matching techniques that iteratively place as closely as possible the 3D facial surfaces by minimizing a distance metric.[1-3] However, these techniques maintain the sensitivity to facial expression and large changes in pose.

In order to facilitate recognition by means of scans matching with large amounts of data, it is more advantageous to extract features from the 3D faces.[4-6] An attractive solution to this problem is to extract geometric information from rigid parts of the face: region ensemble approaches are robust against facial expression changes as well as to partial occlusions.[5-7] The shapes of eye socket and nasal region do not change as much as other regions such as cheeks and mouth during expressions. So, the features extracted from these rigid distinctive regions are used in this work.

We introduce a method for 3D face recognition exploiting the local curvature information, which is a measure that has a high discriminant capability and is robust to deformations as rotation and scaling. In addition, our approach uses conformal representation of facial surfaces in order to preserve angles of the original face surface while simplifies the matching problem.

In general, the proposed algorithm consists of the following stages: before face recognition techniques are applied, surfaces are filtered and faces are segmented; next step is alignment of faces and extraction of curvature based features; then, a conformal parameterization of the original facial surfaces onto a Riemannian manifold is performed; finally, regions

Further author information:
*becheaga@cicese.edu.mx
**vkober@cicese.mx

Optics and Photonics for Information Processing IX, edited by Abdul A. S. Awwal, Khan M. Iftekharuddin, Mohammad A. Matin, Mireya García Vázquez, Andrés Márquez, Proc. of SPIE Vol. 9598, 95980V

which are almost expression-invariant are extracted, and different matching algorithms are utilized. Experimental results are presented using 3D CASIA[A] and Gavab[B] database, which contains significant amount of expression and pose variations.

This paper is organized as follows. The proposed methodology for 3D face recognition is presented in section 2, the data is described in section 3, experimental results are shown in section 4, and finally, conclusions of this work are given in section 5.

2. RECOGNITION ALGORITHM

Preprocessing

Acquisition systems usually contain noisy 3D face scans, therefore we applied a median filter to remove spikes without changing properly scanned points. Then, filtered 3D data were aligned[8] with respect to a neutral face and fed into the next stage in order to perform segmentation and calculation of facial surface curvatures.

In most databases 3D scans are composed of pointclouds that contain a larger area than faces take. In order to crop the faces, the tip of the nose must be located. Usually, the nose tip is the point with the maximum depth value, but in reality this is true only in frontal images. To solve this issue, we use a shape index (SI)[9] to detect the nose tip in each facial scan. This measure assigns values from the interval $[0,1]$ to each 3D point of the face: the low values of the shape index represents a spherical cup while the high values represents a spherical cap. Specifically, there are well-known shape types for five values of the shape index: spherical cup ($SI = 0$), rut ($SI = 0.25$), saddle ($SI = 0.5$), ridge ($SI = 0.75$) and spherical cap ($SI = 1$). The aim of using this shape descriptor is take advantage of its scale independency.

The nose tip appears as a convex point on facial surfaces, which corresponds to a vertex with SI near to 1. When potential candidates are selected, the nose vertex is taken as a point with largest z-value detected by these steps and, finally, the points that fall within a sphere centered on it are retain. Once the faces are cropped, the meshes are triangulated and smoothed, and their 3D geometric information is captured by calculation of the mean curvature.[10]

Next step in our approach is parameterization:[11] the computing of correspondence between the discrete triangulated facial surfaces $\mathcal{X}$ and a homeomorphic planar mesh such that each node of the original 3D mesh is assigned a pair of coordinates (u, v) in the planar region $\mathcal{U}$ (see Fig. 1).

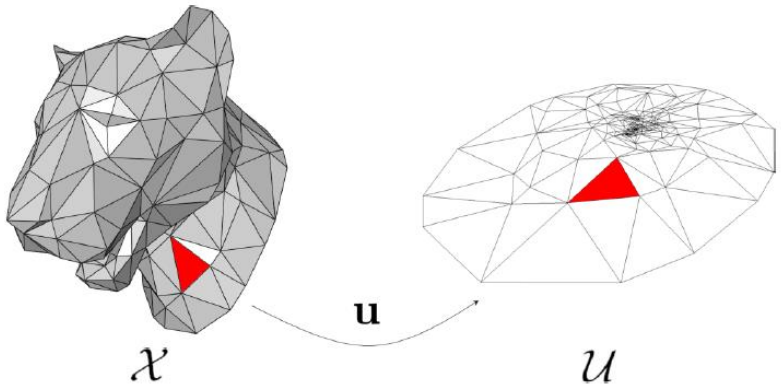

Figure 1. A parameterization $\boldsymbol{u}$ maps each triangle of $\mathcal{X}$ to a planar mesh $\mathcal{U}$ from $\mathbb{R}^3$ to $\mathbb{R}^2$.

[A] http://biometrics.idealtest.org/

[B] http://www.gavab.etsii.urjc.es/recursos.html#GavabDB/

Notation

In this work we consider facial surfaces without holes or possible internal boundaries. We denote $\boldsymbol{u}_i = (u_i, v_i)$ the corresponding 2D position in $\mathcal{U}$ of the *i*-th node of a mesh $\mathcal{X}$. The vector $\boldsymbol{u}$ denotes the column vector $(u_1, v_1, u_2, v_2, \dots, u_V, v_V)^T$, where V is the number of vertices in the mesh. Also, e_{ij} denotes the edge in $\mathcal{U}$ between the vertices u_i and u_j.

Conformal mapping

To introduce the problem of conformal parameterization, we must present the *Dirichlet energy*[12] as a distortion measure that the map $\boldsymbol{u}$ creates. Considering a differential surface patch $\mathcal{X}$ (i.e., a simply connected 2-manifold with boundary) and a smooth map $\boldsymbol{u}$ to $\mathcal{U}$, its Dirichlet energy is defined as the $\mathcal{L}^2$ norm of its gradient,

$$E_D = \frac{1}{2}\int_X |\nabla \boldsymbol{u}|^2 dA. \tag{1}$$

If the minimum value of the Dirichlet energy (i.e. area of the map image) is achieved, the map is *conformal* (also referred to as angle-preserving). In order to measure the difference between E_D and the area of the map image $\mathcal{A}(u) = \int_X \det(\boldsymbol{u})\, dA$, it is convenient to define the conformal energy,

$$E_C(\boldsymbol{u}) = E_D(\boldsymbol{u}) - \mathcal{A}(\boldsymbol{u}), \tag{2}$$

so that now a map $\boldsymbol{u}$ is conformal iff this energy is zero.

Discretization of the map

To adapt the previous concepts to triangle meshes, only the map $\boldsymbol{u}$ needs to be discretized by considering that it maps each triangle on $\mathcal{X}$ to a triangle in $\mathcal{U}$. In this case, Dirichlet energy can be expressed as

$$E_D(\boldsymbol{u}) = \sum_{e_{ij}} \frac{1}{4}\left(\cot(\theta_{ij}) + \cot(\theta_{ji})\right)\left(\boldsymbol{u}_i - \boldsymbol{u}_j\right)^2, \tag{3}$$

where θ_{ij} and θ_{ji} are two angles opposite to the edge linking x_i and x_j on the mesh $\mathcal{X}$. As it is quadratic in the coordinates of $\mathcal{U}$, it can be also described in matrix form as

$$E_D(u) = \frac{1}{2}\boldsymbol{u}^t L_D \boldsymbol{u}, \tag{4}$$

where L_D is a $2V \times 2V$ sparse, symmetrix matrix containing only the cotangent coefficients computed on $\mathcal{X}$.

On other hand, the area of the parameterization can be calculated adding the area $\mathcal{A}_T$ of each mapped triangle *T* in $\mathcal{U}$ with $\mathcal{A}_T(\boldsymbol{u}) = \sum_{e_{ij}\in T} \frac{1}{2}\left(u_i v_j - u_j v_i\right)$. As the internal edges cancel out, the total area can be computed in terms of the coordinates of the boundary vertices as follows:

$$\mathcal{A}(\boldsymbol{u}) = \sum_{e_{ij}\in \partial\mathcal{U}} \frac{1}{2}\left(u_i v_j - u_j v_i\right), \tag{5}$$

where e_{ij} is in the boundary $\partial\mathcal{U}$.

Then, we can define a matrix A such that $\mathcal{A}(\boldsymbol{u}) = \frac{1}{2}\boldsymbol{u}^t A \boldsymbol{u}$. This $2V \times 2V$ matrix is symmetric and extremely sparse, as only the entries corresponding to boundary vertices are non-zero. Consequently, the conformal energy $E_C = E_D - \mathcal{A}$ can be expressed as the quadratic form:

$$E_C(\boldsymbol{u}) = \frac{1}{2}\boldsymbol{u}^t L_C \boldsymbol{u}, \tag{6}$$

where $L_C = L_D - A$. In this form, the map is called discrete conformal when it minimizes the discrete quadratic energy $E_C(\boldsymbol{u})$.

Spectral Conformal Parameterization (SCP)

To solve the minimization of the conformal energy, the discrete spectral conformal parameterization[11] $\boldsymbol{u^*}$ exploits a generalized eigenvector of the following expression:

$$L_c \boldsymbol{u} = \lambda B \boldsymbol{u}, \tag{7}$$

where B is $2V \times 2V$ diagonal matrix with unity at each diagonal element corresponding to boundary vertices and 0 everywhere else. The eigenvalue problem corresponds to the constrained minimization is written as follows:

$$\begin{gathered} \boldsymbol{u}^* = \arg\min_{\boldsymbol{u}} \boldsymbol{u}^t L_C \boldsymbol{u} \\ \boldsymbol{u}^t B \boldsymbol{e} = 0 \\ \boldsymbol{u}^t B \boldsymbol{u} = 1 \end{gathered} \tag{8}$$

where the $2V \times 2V$ matrix **e** is such that $e_{i,1}$ (resp. $e_{i,2}$) is unity for each *u*-coordinate (resp. *v*-coordinate) and 0 otherwise.

The advantage of this approach is that unlike other free-boundary linear methods, this one does not require point constraints, which reduce the typical distortion caused by this method[12-14]. It finds an eigenvector rather than solving a linear system directly. Additionally, the spectral parameterization maximizes the squared distance from boundary vertices to their barycenter over the unit ball defined by the conformal energy.

In this work we use Matlab Mesh Toolkit[C] to compute the spectral conformal parameterization. This toolbox uses the *eigs* function from the Matlab library to find eigenvalues and their associated eigenvector to solve the problem. The *embedSCP* function also implements enforcing insensitivity to sampling irregularity[11] that weights the area from each triangle by the inverting its original area |T| (see Fig. 2),

$$A_{u_i,v_j} = \frac{1}{2}\left(\frac{1}{|T_{ijk}|} - \frac{1}{|T_{ijl}|}\right), A_{v_i,u_j} = \frac{1}{2}\left(-\frac{1}{|T_{ijk}|} + \frac{1}{|T_{ijl}|}\right). \tag{9}$$

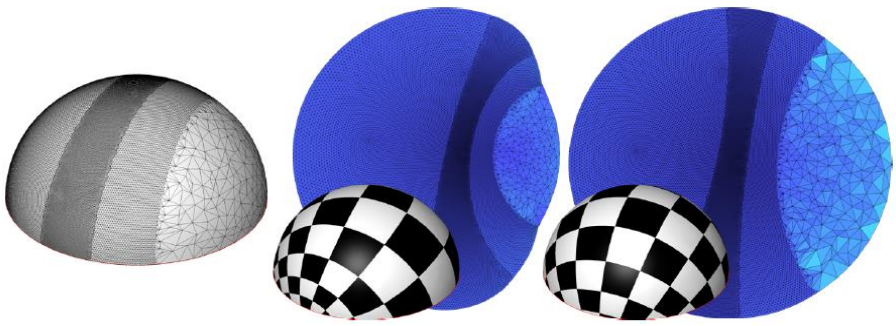

Figure 2. Triangulated face (left); Spectral conformal parameterization without (center) and with (right) area weighting.

[C] http://www.dgp.toronto.edu/~rms/software/matlabmesh/

Data

The Gavab database comprises 3D facial scans with pose and expression variations. We consider the scans of 30 subjects. For each person, we take two frontal scans under neutral expression (N), three scans with expressions (E) and four scans with variation of posture (P). The expressions considered are a random gesture, laugh and smile. The postures variations are looking to the right and to the left and looking up and down.

The CASIA database contains 3D facial scans with larger pose variations and stronger expressions. We consider the scans of 30 subjects. For each person, we take two frontal scans under neutral expression (N), four scans with expressions (E) and four scans with variation of posture (P). The expressions considered are smile, anger, surprise, and eyes closed (under office light and front pose). The postures variations are looking to the right and to the left with a rotation of 20-30 degrees and looking up and down with 20-30 degrees.

3. RESULTS

Experiments description

We applied Principal Component Analysis (PCA) and Linear Discriminant Analysis (LDA) to perform recognition. To perform the PCA, database should be divided into two parts: training set and test set. In our experiments, we form the training set I with a neutral expression model, set II with two neutral expression models and set III with a neutral and a smile model of 30 subjects in the dataset.

Two experiments were performed to prove the effectiveness of our method. The first experiment verifies the effectiveness of using curvature information, segmentation and spectral parameterization with and without weighting over the triangle areas. In order to perform normalization, the tip of the nose on the conformal parameterization was located, the central part of the face was extracted and the data were mapped to the unit circle (Fig. 3). The test set in this experiment contains all the neutral and expression models of our databases which are not included in the training set (Fig. 4). Results are shown in Table 1.

Table 1. Recognition results of PCA-LDA in neutral and expression models of the datasets considering the train set I. Performing is verified using combinations of mean curvature information, segmentation of central face region and spectral conformal parameterization (SCP) with and without weighting.

	Training set	3D information	SCP	SCP w/weight	Mean Curvature	Segmentation	Recognition
CASIA	I		✓			✓	68
	I		✓		✓	✓	66
	I			✓			64
	I			✓	✓		**82.66**
	I			✓	✓	✓	63.33
	I	✓				✓	73
Gavab	I			✓			71.66
	I			✓	✓		**90.83**
	I			✓	✓	✓	65.83
	I	✓					87.5

The results of the first experiment shows that the combination of spectral conformal parameterization with weighting and mean curvature information has the best ability to discriminate between faces among the methods considered on the two datasets (Table 1). Since the segmentation yields a poor performance, we conclude that the normalization stage was not carried out properly.

The second experiment shows the effectiveness of the use of information that had the best performance in Experiment 1 in the presence of pose variations. Again, different training sets (1-3) are considered and the test sets contains all the neutral and expression models not included in the training sets or only pose models. Results are shown in Table 1.

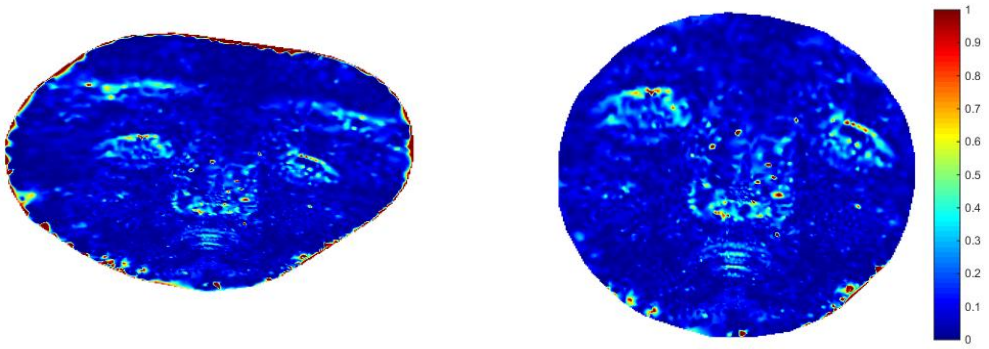

Figure 3. Example of neutral facial scan on CASIA database before (left) and after (right) segmentation of central face region showing mean curvature information over spectral conformal parameterization.

The results of the second experiment shows that the discrimination capability of the combination of mean curvature and spectral conformal parameterization can be improved by adding more facial models to the training set. Moreover, further improvement can be achieved, if expression models are considered (Table 2).

Table 2. Recognition results of PCA-LDA in neutral (N), expression (E) and pose models (P) of the datasets using neutral sets (I,II) and expression set (III) models as training. Performing is verified using combinations of mean curvature information, segmentation of central face region and spectral conformal parameterization (SCP) with and without weighting.

	Training set	SCP w/weight	Curvature	Test set		Recognition
				N+E	P	
CASIA	I	✓	✓	✓		82.66
	II	✓	✓	✓		93
	III	✓	✓	✓		90
	II	✓	✓		✓	87.5
	III	✓	✓		✓	83.33
Gavab	II	✓	✓	✓		100
	III	✓	✓	✓		96.66
	I	✓	✓		✓	76.66
	II	✓	✓		✓	84.16
	III	✓	✓		✓	85

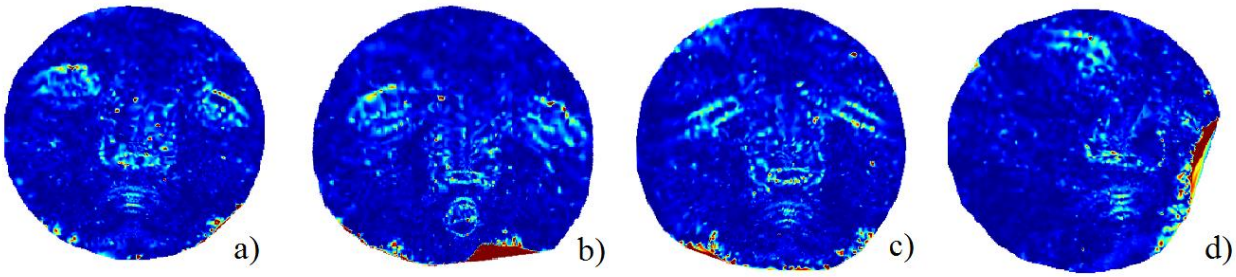

Figure 4. Example of spectral conformal parameterization in (a) neutral, (b) surprise, (c) eyes closed and (d) pose variation model in CASIA database.

CONCLUSIONS

In this paper, we propose a recognition algorithm which deals with expressions and pose variation employing spectral conformal parameterization in order to preserve angles of the original face surface while simplifies the matching problem. In addition, our approach uses local curvature information, which is a measure with high discriminant capability and has the advantage of being robust to deformations as rotation and scaling.

The results obtained from the experiments shown that the combination of spectral conformal parameterization and mean curvature information has the best performance.

Future work includes considering larger datasets and improvement of the algorithm to increase the recognition rate adding models to training sets.

ACKNOWLEDGMENTS

The work was supported by Russian Science Foundation grant №15-19-10010.

REFERENCES

[1] Lee, Y. H., Shim, and J. C., “Curvature based human face recognition using depth weighted hausdorff distance,” Proc. ICIP 3, 1429-1432 (2004).

[2] Mian, A. S., Bennamoun, M., and Owens, R., “Keypoint detection and local feature matching for textured 3D face recognition,” Int. J. Comput. Vis. 79(1), 1-12 (2008).

[3] Smeets, D., Claes, P., Hermans, J., Vandermeulen, D., and Suetens, P., “A comparative study of 3-D face recognition under expression variations,” IEEE Trans. Syst. Man, Cybern. Part C (Applications Rev.) 42(5), 710-727 (2012).

[4] Lu, X., and Jain, A. K., “Deformation modeling for robust 3D face matching,” IEEE Trans. Pattern Anal. Mach. Intell. 30(8), 1346-1357 (2008).

[5] Al-Osaimi, F., Mohammed Bennamoun, and Ajmal Mian., "An expression deformation approach to non-rigid 3D face recognition," Int. J. Comput. Vis. 81(3), 302-316 (2009).

[6] Alyuz, N., Gokberk, B., and Akarun, L., “A 3D face recognition system for expression and occlusion invariance,” Proc. BTAS, 1-7 (2008).

[7] Queirolo, C. C., Silva, L., Bellon, O. R., and Pamplona Segundo, M., "3D face recognition using simulated annealing and the surface interpenetration measure," IEEE Trans. Pattern Anal. Mach. Intell. 32(2), 206-219 (2010).
[8] Rusinkiewicz, S., and Levoy, M., "Efficient variants of the ICP algorithm," Proc. IEEE 3DIM, 145-152 (2001).
[9] Szeptycki, P., Ardabilian, M., and Chen, L., "A coarse-to-fine curvature analysis-based rotation invariant 3D face landmarking," Proc. BTAS, 1-6 (2009).
[10] Meyer, M., Desbrun, M., Schroder, P., and Barr, A.H., "Discrete differential-geometry operators for triangulated 2-manifolds," Proc. of Vis. Mat., 35-57 (2003).
[11] Mullen, P., Tong, Y., Alliez, P., and Desbrun, M., "Spectral conformal parameterization," Comput. Graph. Forum 27(5), 1487-1494 (2008).
[12] Wang, S., Wang, Y., Jin, M., Gu, X. D., and Samaras, D., "Conformal geometry and its applications on 3D shape matching, recognition, and stitching," IEEE Trans. Pattern Anal. Mach. Intell. 29(7), 1209-1220 (2007).
[13] Zeng, W., and Gu, X. D., "Surface matching and registration using symmetric conformal mapping," IEEE CAD/Graphics, 249-254 (2009).
[14] Lévy, B., Petitjean, S., Ray, N., and Maillot, J. "Least squares conformal maps for automatic texture atlas generation," ACM Trans. Graphics 21(3), 362-371 (2002).